Climate Effects of Black Carbon Aerosols in China and India

Surabi Menon, *et al.*

Climate Effects of Black Carbon Aerosols in China and India

Surabi Menon,[1,2]* James Hansen,[1] Larissa Nazarenko,[1,2] Yunfeng Luo[3]

In recent decades, there has been a tendency toward increased summer floods in south China, increased drought in north China, and moderate cooling in China and India while most of the world has been warming. We used a global climate model to investigate possible aerosol contributions to these trends. We found precipitation and temperature changes in the model that were comparable to those observed if the aerosols included a large proportion of absorbing black carbon ("soot"), similar to observed amounts. Absorbing aerosols heat the air, alter regional atmospheric stability and vertical motions, and affect the large-scale circulation and hydrologic cycle with significant regional climate effects.

China has been experiencing an increased severity of dust storms, commonly attributed to overfarming, overgrazing, and destruction of forests (*1*). Plumes of dust from north China, with adhered toxic contaminants, are cause for public health concern in China, Japan, and Korea, and some of the aerosols even reach the United States (*2*). Recent dust events have prompted Chinese officials to consider spending several hundred billion yuan (~\$12 billion) in the next decade to increase forests and green belts to combat the dust storms (*3*). Such measures may be beneficial in any case. However, we suggest that the observed trend toward increased summer floods in south China and drought in north China (*4*), thought to be the largest change in precipitation trends since 950 A.D. (*4*), may have an alternative explanation: human-made absorbing aerosols in remote populous industrial regions that alter the regional atmospheric circulation and contribute to regional climate change. If our interpretation is correct, reducing the amount of anthropogenic black carbon aerosols, in addition to having human health benefits, may help diminish the intensity of floods in the south and droughts and dust storms in the north. Similar considerations may apply to India and neighboring regions such as Afghanistan, which have experienced recent droughts.

Atmospheric aerosols, which are fine particles suspended in the air, comprise a mixture of mainly sulfates, nitrates, carbonaceous (organic and black carbon) particles, sea salt, and mineral dust. Black (elemental) carbon (BC) is of special interest because it absorbs sunlight, heats the air, and contributes to

global warming (*5*, *6*), unlike most aerosols, which reflect sunlight to space and have a global cooling effect (*7*). BC emissions, a product of incomplete combustion from coal, diesel engines, biofuels, and outdoor biomass burning (*8*), are particularly large in China and India because of low-temperature household burning of biofuels and coal (*9*).

It is reasonable to anticipate that human-made aerosols may contribute to climate change in China and India, because both absorbing BC aerosols and reflective aerosols, such as sulfates, reduce the amount of sunlight reaching the ground and thus should tend to cause local cooling. Observed temperatures in China and India in recent decades, unlike most of the world, reveal little warming (*10*); and in some seasons there is cooling, especially in the summer when aerosol effects should be largest. The climate effect of aerosols is complicated, because aerosols have, in addition to their direct radiative effects, indirect effects on cloud properties (*7*, *11*).

Here we report on climate model simulations of the direct radiative effect of aerosols in the region of China and India. We used the Goddard Institute for Space Studies (GISS) SI2000 12-layer climate model, which has been used to study the impact of several forcings on global mean temperature (*12*). Figure 1 shows the (seasonally independent) added aerosol optical depth $\Delta\tau_{aer}$ (0.55 μm) used in our climate model experiments (*13*). Over China, we take $\Delta\tau_{aer}$ (0.55 μm) to be equal to τ_{aer} (0.75 μm) measured in the 1990s (*14*, *15*). Over India and the Indian Ocean, $\Delta\tau_{aer}$ in our experiments is taken from chemical transport model assimilations of satellite measurements (*16*). The resulting radiative forcings at the top of the atmosphere and surface (fig. S1) are ~+6 W m^{-2} and –17 W m^{-2}, respectively, over India and the Indian Ocean, which is comparable to values estimated by others (*17*).

We performed two primary experiments. In experiment A, we added the aerosols of

Fig. 1 with aerosol single-scatter albedo (SSA) = 0.85 (*18*), which is representative of measurements from the Indian Ocean Experiment (INDOEX) (*17*) and industrial regions in China. We obtained such relatively "dark" aerosols by including an appropriate amount of BC, with the remainder being sulfate. In experiment B, we removed BC so that SSA = 1; i.e., the aerosols were "white." In both A and B, the sea surface temperature (SST), greenhouse gases, and other forcings were kept fixed at the same values as in the control run, so that the aerosols were the only forcing. Both experiments were run for 120 years.

Figure 2A shows the simulated summer [June, July, and August (JJA)] surface air temperature (T_S) changes. The aerosols with SSA = 0.85 yield cooling in China by 0.5 to 1 K (a consequence of the reduced solar radiation reaching the surface) but warming in most of the world [due to BC heating of the troposphere (*19*)]. Because of the long model run, the cooling in China and even the warming in many distant locations are highly significant (>99%), based on Student's *t* test (fig. S2). The simulated cooling in China is larger than the observed cooling there during the past 50 years (Fig. 2B), when most of the increase in aerosol amount probably occurred. This is as expected, because the simulations exclude the effect of increasing greenhouse gases (*20*).

The BC absorption in China and India causes a significant warming (>0.5 K) in the Sahara Desert region and in west and central Canada, despite the fixed SST. Because aerosols were unchanged outside the China/India region, this warming at a distance seems to be due to heating of tropospheric air over China and India, with dynamical export to the rest of the world, where the warmer troposphere can reduce convective and radiative cooling of the surface. Consistent with observations (*10*, *21*), this warming does not occur over the south central United States, where the observed cooling trend is thought to be driven by warming in the tropical Pacific Ocean (*21*, *22*).

Aerosol optical depth
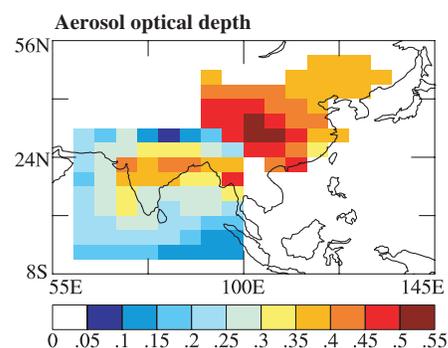
Fig. 1. Incremental aerosol optical depth $\Delta\tau_{aer}$ (0.55 μm), which is used to drive the climate change simulations. Latitude and longitude are denoted.

[1]NASA Goddard Institute for Space Studies, New York, NY 10025, USA. [2]Center for Climate Systems Research, Columbia University, New York, NY 10025, USA. [3]National Science Foundation of China, Haidian, China.

*To whom correspondence should be addressed. E-mail: smenon@giss.nasa.gov

Experiment B, with pure sulfate aerosols, yields global cooling (Fig. 2A) as expected, but the cooling in China is small compared with that in experiment A. The difference is that BC heats the air, thus increasing local convection, precipitation, and surface cooling, as we illustrate below. The sulfate aerosols are ineffective at causing global cooling ($\Delta T_S = -0.03$K) when SSTs are fixed. Reflective aerosols become an efficacious forcing when feedback effects such as sea ice cover are allowed to operate (19).

Figure 3 shows simulated summer (JJA) precipitation changes. The aerosols with SSA = 0.85 yield increased precipitation in southern China and over India and Myanmar where $\Delta\tau_{aer}$ was largest. There is a broad band of decreased precipitation to the south of the region with increased precipitation, with a lesser decrease to the north. The magnitude of the precipitation changes, ~0.5 mm/day or 5 cm for the season, is comparable to changes based on observed trends over several decades (4). In comparison, precipitation changes are small in experiment B and, contrary to observations, no increase is found over south China. Further, simulation of greenhouse gas effects with the same climate model (12), but without the strong BC aerosol absorption, yields warming throughout China, with increased rainfall in the north and decreased rainfall in the southeast, all contrary to observations.

Climate change simulations are most meaningful if the model's climatology reproduces observed regional climate patterns. The GISS model reproduces features of the large-scale circulation associated with the Asian summer monsoon, such as southwesterly winds bringing moisture to eastern China from the Indian Ocean and South China Sea, upper-level westerlies and an anticyclone centered over the Tibetan Plateau, and strong upper-level easterlies south of the plateau; but, in common with other models, it does not reproduce the strength of northwesterly surface winds in the western Pacific (23). Also in common with most models, it does not accurately reproduce regional precipitation patterns and their seasonal shifts (24), but this should not prevent the model from producing meaningful large-scale changes over polluted industrial China (the southern half of China) relative to regions to the north and south and to distant global regions.

The circulation changes in experiments A and B are dramatically different. Experiment A yields stronger upper-level westerlies to the north and easterlies to the south of the Tibetan Plateau, whereas in B the anticyclone is weakened and westerlies are present south of the plateau. We do not have real-world data on long-term trends that allow us to discriminate between absorbing aerosols (A) and white aerosols (B).

The reason why a relatively small proportion of BC aerosols can play such a dominant role in the aerosol climate effect derives not only from the reduction in surface solar radiation but also from the heating of the air and the effects of these on the vertical temperature profile, evaporation, latent heat fluxes, atmospheric stability, and the strength of convection. Changes in convection, in turn, can modify the large-scale circulation (25). This is illustrated in the change of vertical velocity averaged over 90° to 130°E (an area with large $\Delta\tau_{aer}$) (Fig. 4). There are increased rising motions over the area of added aerosols, with comparable increased subsidence to the south and weaker subsidence to the north.

As a check on our interpretation of these experiments, we carried out additional related experiments. In experiment C, we included only the increase of BC aerosols; that is, the sulfates and other aerosols were identical to those in the control run. Experiment C yielded results similar to A, even though the larger part of $\Delta\tau_{aer}$ of A was excluded, confirming that BC aerosols are the driver for the results. Results for T_S and precipitation changes from experiment C are in fig. S4.

Another experiment (D) was performed to check whether observed changes in T_S and precipitation in China might be associated more with changes in ocean temperatures around China than with aerosols. In experiment D, SST (and sea ice) anomalies were added to the control run corresponding to the observed changes that occurred over the past 50 years. The resulting climate changes over China were small in comparison to those in experiment A, and the precipitation changes

Fig. 2. (**A**) Simulated JJA surface air temperature change (ΔT_S) for experiments A and B. The significance of these changes is shown in fig. S2. (**B**) Observed JJA ΔT_S between 1951 and 2000, based on the linear trend. Global mean changes are in the upper right corner.
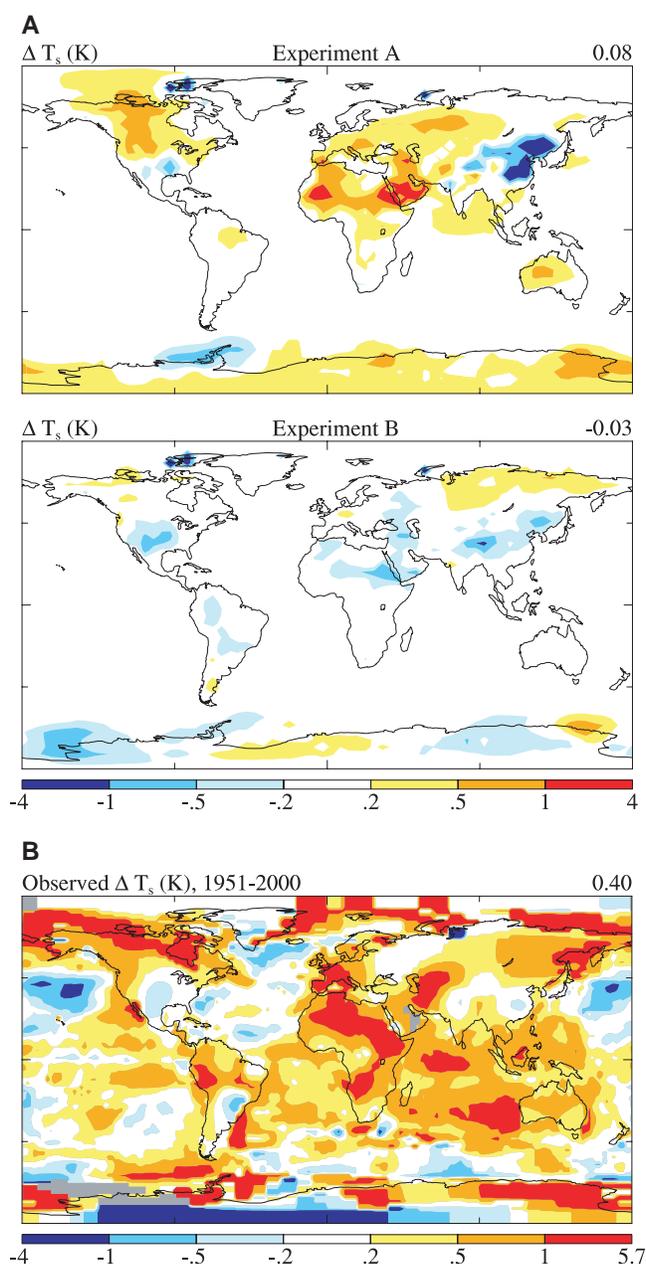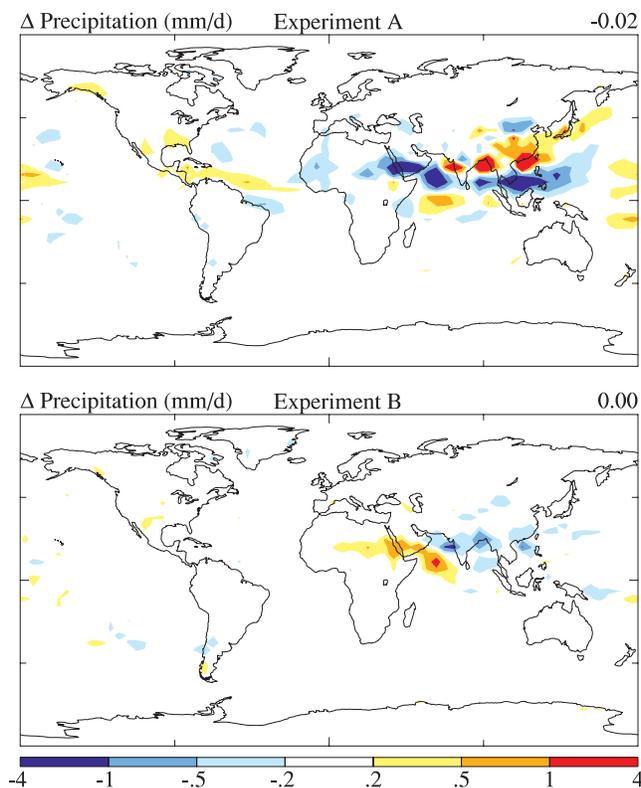
2251

Fig. 3. Same as Fig. 2A, but for precipitation. The significance of these changes is shown in fig. S3.

Δ Precipitation (mm/d) Experiment A -0.02

Δ Precipitation (mm/d) Experiment B 0.00

-4 -1 -.5 -.2 .2 .5 1 4

Δw (10⁻⁵ hPa/s) Experiment A

-23 -15 -10 -5 -1 -.5 .5 1 5 10 15 20

Fig. 4. Simulated JJA vertical velocity change (Δw), as a function of latitude and height, averaged over 90° to 130°E for experiment A.

(a small decrease in south China) and temperature changes (summer warming in China) (fig. S5) were contrary to observations.

One climate impact of the aerosols in our experiments that disagrees with observations is the simulated cloud cover change (fig. S6) for experiment A. The modeled cloud cover increases in the region with added aerosols by as much as several percent. Globally there is a decrease in cloud cover, especially in the regions with surface air warming, which is consistent with the expected "semi-direct" effect of absorbing aerosols on global cloud cover (19). We cannot verify the global effect because of the many forcings in other parts of the world and the limited accuracy of information on global cloud cover. However, we can compare the large simulated changes in China and the Indian Ocean with observations.

The simulated increase of cloud cover over China in experiment A is contrary to observations from 1951–1994 (26) that show a decrease of ~1 to 3% in the north and insignificant changes in the south. Observations of long-term cloud cover change are difficult, and the decreasing amplitude of the diurnal cycle of T_S, arguably a proxy measure of cloud cover change, suggests a cloud cover increase over China (27). Nevertheless, it seems clear that a cloud cover increase as large as that simulated in experiment A has not occurred in recent decades (28).

Over the Indian Ocean, our simulated low cloud cover increase is consistent with the low cloud cover trend observed between

1952 and 1996 (29). This is contrary to the decrease of trade cumulus clouds over the Indian Ocean found in a large-eddy simulation model when solar heating from soot was taken into account (30, 31). It has been argued that the increase in clouds over the Indian Ocean may be related to an increase of SST, which causes increased evaporation and buoyancy that might minimize the drying effect of BC heating (29). In our model, however, the increased cloud cover over the Indian Ocean is due to increased vertical motions driven by aerosol heating, similar to the changes over China.

We believe that our primary conclusions are not dependent on the uncertainties about the nature and origin of cloud cover changes. As a test of this hypothesis, we performed an experiment E with the same aerosols as in A, but with the cloud cover held fixed by using clouds from the control run. The results of this experiment were qualitatively similar to those in A, with cooling and increased precipitation over China (fig. S7).

We conclude that absorbing aerosols can affect regional climate, and we suggest that precipitation trends in China over the past several decades, with increased rainfall in the south and drought in the north, may be related to increased BC aerosols, though we do not discount the possibility that land use and water resource policies also contribute to observed droughts. Observations do not show obvious large-scale climate trends over India, but we speculate that the increase of dark carbon-rich
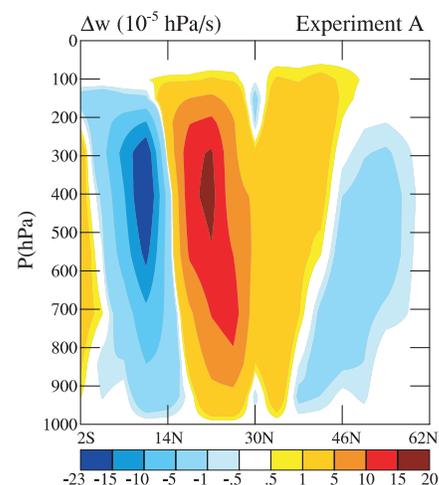
aerosols in India (8) could contribute to a tendency toward increased droughts in northern areas, such as Afghanistan, as well as to climate changes in India. The coarse resolution of our model (4° × 5°) and the absence of an Indian network of aerosol measurements comparable to that in China (14) make it difficult to define a realistic aerosol change in India (32).

The regional climate effects of black carbon aerosols, if confirmed by further studies, provide another reason to reduce this anthropogenic air pollution. Black carbon also contributes significantly to global warming (5, 6), and it has been suggested that soot aerosols, which include both black and organic carbon, are carcinogenic and are a major cause of deaths associated with particulate air pollution (33). Much more needs to be known about the composition specificity of aerosol climate and health effects. However, there is mounting evidence that black carbon may be a particularly "bad actor."

References and Notes
1. H. W. French, *New York Times*, 14 April 2002, p. 3.
2. R. B. Husar *et al.*, *J. Geophys. Res.* **106**, 18317 (2001).
3. Reuters, http://in.news.yahoo.com/020514/64/1o02h.html, 14 May 2002.
4. Q. Xu, *Atmos. Environ.* **35**, 5029 (2001).
5. J. Hansen, M. Sato, R. Ruedy, A. Lacis, V. Oinas, *Proc. Natl. Acad. Sci. U.S.A.* **97**, 9875 (2000).
6. M. Jacobson, *Nature* **409**, 695 (2001).
7. J. E. Penner *et al.*, in *Climate Change 2001: The Scientific Basis*, J. T. Houghton *et al.*, Eds. (Cambridge Univ. Press, Cambridge, 2001), pp. 289–348.
8. T. Novakov *et al.*, *Geophys. Res. Lett.* **27**, 4061 (2000).
9. D. G. Streets *et al.*, *Atmos. Environ.* **35**, 4281 (2001).
10. J. Hansen *et al.*, *J. Geophys. Res.* **106**, 23947 (2001).
11. Previous studies of aerosol effects on regional climate have used satellite data to study the role of smoke particles in clouds in Amazonia [Y. J. Kaufman, R. S. Fraser, *Science* **277**, 1573 (1997)] and the effect of aerosols in suppressing precipitation: dust in the eastern Mediterranean [D. Rosenfeld, Y. Rudich, R. Lahav, *Proc. Natl. Acad. Sci. U.S.A.* **98**, 5975 (2001)] and sulfates in the Sahel [L. D. Rotstayn, U. Lohmann, *J. Clim.* **15**, 2103 (2002)].
12. J. Hansen *et al.*, *J. Geophys. Res.*, in press.

13. The control run of the GISS model used in our experiments has atmospheric composition estimated for 1951, with an aerosol optical depth (τ_{aer}) over India and China ~ 0.1 at wavelength $\lambda = 0.55$ μm [figure 8 of (12)].

14. Y. Luo, L. Daren, X. Zhou, W. Li, Q. He, *J. Geophys. Res.* **106**, 14501 (2001).

15. Surface solar radiation observations have been used to estimate aerosol optical depth at 0.75 μm (14). This optical depth includes both the natural and anthropogenic components. We use this optical depth to approximate the anthropogenic aerosol optical depth at 0.55 μm. Because aerosol optical depth varies approximately as λ^{-1} or slightly faster, this corresponds to an assumption that about two-thirds of current aerosols in China are anthropogenic, which is probably not a great exaggeration.

16. W. D. Collins *et al.*, *J. Geophys. Res.* **106**, 7313 (2001).

17. V. Ramanathan *et al.*, *J. Geophys. Res.* **106**, 28371 (2001).

18. The effective SSA for solar radiation is about 0.85. Resulting atmospheric absorption over south China (20° to 36°N, 90° to 130°E) is 24 Wm^{-2} (+6 W m^{-2} at the top of the atmosphere and -18 W m^{-2} at the surface), causing an increase in atmospheric heating by as much as 0.3 K/day in the lower troposphere. A value of 0.9, instead of 0.85, would imply about one-third less absorption, thus decreasing the magnitude of temperature and precipitation changes that we obtain in experiment A.

19. J. Hansen, M. Sato, R. Ruedy, *J. Geophys. Res.* **102**, 6831 (1997).

20. Observed global warming is about 0.5 K in the past 50 years (10), as is simulated global and regional warming due to increasing greenhouse gases (12). Thus the magnitude of our simulated aerosol cooling is consistent with observations.

21. W. A. Robinson, R. Ruedy, J. E. Hansen, *J. Geophys. Res.*, in press.

22. The cooling that we find in our experiment A for the south central United States (Fig. 2A) is consistent with the calculated warming of the troposphere over the tropical Pacific Ocean.

23. K.-M. Lau, M.-T. Li, *Bull. Am. Meteorol. Soc.* **65**, 114 (1984).

24. K.-M. Lau, J. H. Kim, Y. Sud, *Bull. Am. Meteorol. Soc.* **77**, 2209 (1996).

25. D. A. Randall, Harshvardhan, D. A. Dazlich, T. G. Corsetti, *J. Atmos. Sci.* **46**, 1943 (1989).

26. D. P. Kaiser, *Geophys. Res. Lett.* **25**, 3599 (1998).

27. B. Sun, P. Ya. Groisman, R. S. Bradley, F. T. Keimig, *J. Clim.* **13**, 4341 (2000).

28. We note that cloud changes in response to climate change are notoriously difficult for climate models to simulate with confidence. In addition, the indirect effect of aerosols on cloud microphysics, which is thought to cause cloud cover to increase, is not included in our simulations. However, the indirect effect of anthropogenic aerosols on clouds may have been partially saturated by the time the cloud cover observations originated.

29. J. R. Norris, *Geophys. Res. Lett.* **28**, 3271 (2001).

30. A. S. Ackerman *et al.*, *Science* **288**, 1042 (2000).

31. The results from (30) were based on a single meteorological scenario and may be linked to the dynamical conditions prevalent over the Indian Ocean at the time.

32. More precise knowledge of the horizontal and vertical distribution of the aerosols is needed. The vertical distribution affects the radiative heating profile and thus may influence the atmospheric dynamical response to aerosols [M. Jacobson, *J. Geophys. Res.* **103**, 10593 (1998)]. Present global observations do not define the aerosol vertical profile, but future satellite measurements that include lidar and precision polarimetry offer the potential of defining the aerosol height distribution accurately.

33. N. Kunzli *et al.*, *Lancet* **356**, 795 (2001).

34. We thank T. Novakov, A. Hansen, P. Stone, A. Del Genio, C. Jakob, and W. Lau for generous discussions on soot aerosols and climate change. Our research is supported by NASA programs managed by J. Kaye, T. Lee, and E. Lindstrom and by NSF grant 0074176.

A Single P450 Allele Associated with Insecticide Resistance in *Drosophila*

P. J. Daborn,[1] J. L. Yen,[1] M. R. Bogwitz,[2] G. Le Goff,[1] E. Feil,[1] S. Jeffers,[3] N. Tijet,[4] T. Perry,[2] D. Heckel,[2] P. Batterham,[2] R. Feyereisen,[5] T. G. Wilson,[3] R. H. ffrench-Constant[1]*

Insecticide resistance is one of the most widespread genetic changes caused by human activity, but we still understand little about the origins and spread of resistant alleles in global populations of insects. Here, via microarray analysis of all P450s in *Drosophila melanogaster*, we show that *DDT-R*, a gene conferring resistance to DDT, is associated with overtranscription of a single cytochrome P450 gene, *Cyp6g1*. Transgenic analysis of *Cyp6g1* shows that overtranscription of this gene alone is both necessary and sufficient for resistance. Resistance and up-regulation in *Drosophila* populations are associated with a single *Cyp6g1* allele that has spread globally. This allele is characterized by the insertion of an *Accord* transposable element into the 5' end of the *Cyp6g1* gene.

Insecticide resistance represents an important example of natural selection. Resistance can be mediated either by changes in the sensitivity of insecticide targets in the nervous system or by metabolism of insecticides before they reach these targets (1). Insecticide resistance associated with target site insensitivity is well documented within the *para*-encoded voltage-gated sodium channel, the *Rdl*-encoded ligand-gated chloride channel, and the *Ace*-encoded acetylcholinesterase (1). However, the up-regulation of metabolic enzymes associated with resistance, such as the cytochrome P450s and glutathione S-transferases, remains less well understood (2–7). We are using *Drosophila melanogaster* as a model insect in which to dissect the genetic basis of metabolic insecticide resistance (8, 9), particularly at the *DDT-R* locus. This locus not only represents insect resistance to DDT (10), a compound largely withdrawn but still used in the control of disease vectors (11), but also confers cross-resistance to a wide range of other existing and novel insecticides (12–15). *DDT-R* is a dominant gene that maps to the right arm of chromosome II at 64.5 cM (16, 17). Recently, we have shown that *DDT-R* is associated with overtranscription of the P450 gene *Cyp6g1* in three *D. melanogaster* strains (18). In

this study, we were interested in answering three questions. First, is *Cyp6g1* overtranscribed in all P450-mediated DDT-resistant *D. melanogaster* strains? Second, if so, is resistance globally associated with a single resistance allele? Third, is overtranscription of *Cyp6g1* alone both necessary and sufficient for resistance?

The genes for the cytochrome P450s are a large family involved in a wide variety of metabolic functions. In insects, these enzymes play roles in key processes ranging from host plant utilization to xenobiotic resistance (3). Within the complete genome sequence of *D. melanogaster*, some 90 individual P450 genes have been identified (19). To determine the breadth of the correlation between *Cyp6g1* overtranscription and DDT resistance in *D. melanogaster*, we challenged a microarray carrying polymerase chain reaction (PCR) products from all identified P450 open reading frames in the genome. Array analysis of Hikone-R (20), a resistant strain established from field collections in the early 1960s (16, 21), shows that only *Cyp6g1* is overtranscribed relative to Canton-S, a susceptible reference strain (Fig. 1A). Similar array analysis of a second DDT-resistant strain, WC2, which was recently collected in the field (U.S.A.), revealed the same result, with only *Cyp6g1* being overtranscribed relative to P450 gene expression in the susceptible standard (Fig. 1B). To measure the level of overtranscription associated with resistance, we performed quantitative reverse transcriptase (RT)–PCR on mRNA from a range of resistant and susceptible strains (22), relative to the standard *RP49* (23). This analysis confirms the relative overtranscription of *Cyp6g1* in a range of strains and shows 10 to 100 times as much mRNA in resistant strains as in a range of susceptible strains

¹Department of Biology and Biochemistry, University of Bath, Bath BA2 7AY, UK. ²Centre for Environmental Stress and Adaptation Research (CESAR), Department of Genetics, University of Melbourne, Victoria, 3052, Australia. ³Department of Biology, Colorado State University, Fort Collins, CO 80523, USA. ⁴Department of Entomology, University of Arizona, Tucson, AZ 85721, USA. ⁵INRA Centre de Recherches d'Antibes, 1382 Route de Biot, 06560, Valbonne, France.

*To whom correspondence should be addressed. E-mail: bssrfc@bath.ac.uk

2253